Baryon anomaly and strong color fields in Pb + Pb collisions at 2.76A TeV at the CERN Large Hadron Collider

V. Topor Pop,[1] M. Gyulassy,[2] J. Barrette,[1] and C. Gale[1]
[1]*McGill University, Montreal, Quebec, Canada H3A 2T8*
[2]*Columbia University, New York, New York 10027, USA*
(Received 29 June 2011; published 24 October 2011)

With the HIJING/B$\bar{\text{B}}$ v2.0 heavy ion event generator, we explore the phenomenological consequences of several high parton density dynamical effects predicted in central Pb+Pb collisions at the Large Hadron Collider (LHC) energies. These include (1) jet quenching due to parton energy loss (dE/dx), (2) strangeness and hyperon enhancement due to strong *longitudinal* color field (SCF), and (3) enhancement of baryon-to-meson ratios due to baryon-antibaryon junction (J$\bar{\text{J}}$) loops and SCF effects. The saturation/minijet cutoff scale $p_0(s, A)$ and effective string tension $\kappa(s, A)$ are constrained by our previous analysis of LHC $p + p$ data and recent data on the charged multiplicity for Pb+Pb collisions reported by the ALICE collaboration. We predict the hadron flavor dependence (mesons and baryons) of the nuclear modification factor $R_{AA}(p_T)$ and emphasize the possibility that the baryon anomaly could persist at the LHC up to $p_T \sim 10$ GeV, well beyond the range observed in central Au+Au collisions at RHIC energies.

DOI: 10.1103/PhysRevC.84.044909 PACS number(s): 12.38.Mh, 24.85.+p, 25.75.−q, 24.10.Lx

I. INTRODUCTION

With the commissioning of the Large Hadron Collider (LHC), it is now possible to test dynamical models of multiparticle production in nuclear collisions up to a center-of-mass energy (c.m.) per nucleon $\sqrt{s_{NN}} = 5.5$ TeV. Charged particle densities at mid-pseudorapidity, $(2dN_{\text{ch}}/d\eta)/N_{\text{part}}$, and their dependence on energy and centrality are important for understanding the mechanism of hadron production and especially the interplay of soft (string fragmentation) and hard (perturbative quantum chromodynamics) scattering contributions at an order of magnitude higher energies than were extensively studied up to now at the Relativistic Heavy Ion Collider (RHIC/BNL). The rate of parton-parton and multi-parton-parton scattering and soft processes are strongly correlated with the observed particle multiplicity (related to the *initial entropy* and the *initial energy density* generated in nuclear collisions over space-time volumes up to 10^4 greater than in elementary $p + p$ collisions).

Using the constraints on dynamical parameters from data at RHIC energies, there remain relatively large uncertainties ($\sim$ a factor of two) on predictions for charged hadron multiplicities at the LHC energies; see Refs. [1–16]. The first data on inclusive charged particle distributions from the LHC in Pb+Pb collisions are now available [17–22]. Recently, ATLAS analyzed event samples from central (0%–10%) Pb+Pb collisions at $\sqrt{s_{NN}} = 2.76$ TeV in which the transverse energy of the most energetic jet (leading jet) $E_{T_1} > 100$ GeV and where a recoiling jet with transverse energy $E_{T_2} > 25$ GeV could be found at azimuthal separation $\Delta\Phi > \pi/2$. In comparison with pp collisions, ATLAS observed (within a narrow cone) in Pb+Pb collisions a strong reduction of the number of recoiling jets carrying a large fraction of the maximum available jet energy $x = E_{T_2}/E_{T_1} > 0.6$ [21]. This is consistent with the expected strong quenching of jets due to partonic energy loss in ultradense quark gluon plasma (QGP). In addition to the tomographic interest in jet quenching high p_T observables, there is considerable interest on the impact of minijet quenching as an additional final state interaction source of the observed bulk multiplicity/entropy production. The LHC data on nucleus-nucleus ($A + A$) collisions may lead to an improved theoretical understanding of ultradense multiparton plasma based on a quantum chromodynamics (QCD) approach [9,10,23–25].

To isolate quark-gluon plasma signatures in heavy-ion collision data, it is imperative to work in a framework that can simultaneously account for nucleon-nucleon collisions ($p + p$) in the same energy range. In fact $p + p$ reactions cannot be considered as elementary at the LHC and their study has already revealed possible interesting new physics [26]. We utilize the HIJING/B$\bar{\text{B}}$2.0 heavy-ion generator as a phenomenological tool that can systematically relate observables in $p + p$, $p + A$, and $A + A$ collisions in terms of a common framework based on a two-component picture of the dynamics involving soft longitudinal beam jets, multiple minijets, and rare hard pQCD processes. The Monte Carlo code inherits the phenomenological successes of the LUND [27] and dual-parton model (DPM) [28] string excitation and hadronization mechanisms as well as the hard processes encoded in the PYTHIA [29] event generator. Multiple low $p_T < Q_s(x, A)$ transverse momentum color exchanges excite the incident baryons into longitudinal strings that fragment due to color neutralization into an array of physical hadron resonance states. Hard processes are modeled as high p_T kinks in the strings and hadronize via the well-tested LUND scheme in e^+e^- and ep processes. The HIJING model [30] uses a variant of the string excitation LUND and DPM models constrained to lower energy pp data.

In heavy-ion collisions, the novel "nuclear physics" is due to the nuclear modification of the parton distribution functions, the possibility of multiple longitudinal flux tube overlapping leading to strong longitudinal color field (SCF) effects referred to as color ropes or glasma. Strong fields also lead to enhanced

strangeness production [31]. The effect is especially enhanced for production of baryons with multiple strange quarks as discovered first at the SPS/CERN [32]. Recently, the data on the production of strange particles with one, two, or more strange quarks for $p + \bar{p}$ collisions at the Tevatron [33] and for $p + p$ collisions at the LHC [34,35] have been reported. In Ref. [33] it was shown that the ratio Ξ^-/Λ and Ω^-/Λ rise at low p_T and the ratio reaches an unexpected plateau at $p_T > 4$ GeV/c, which persists up to rather large 10 GeV/c. This result is a major motivation for the present work.

We address these and other issues within the framework of the HIJING/B$\bar{\text{B}}$ v2.0 model [36–38]. A systematic comparison with data on $p + p$ and $p + \bar{p}$ collisions in a wide energy range [36] revealed that minijet production and fragmentation as implemented in the HIJING/B$\bar{\text{B}}$ v2.0 model provide a simultaneous and consistent explanation of several effects: the inclusive spectra at moderate transverse momentum ($p_T <$ 5 GeV/c), the energy dependence of the central rapidity density, the (strange) baryon-meson ratios and the baryon-antibaryon asymmetry. Specifically, in this paper we extend our studies to the dynamic consequences of initial and final state saturation phenomena, gluonic J$\bar{\text{J}}$ loops, and jet quenching to particle production in central (0%–5%) Pb+Pb collisions at the LHC. Our study aims to investigate a set of observables sensitive to the dynamics of the collisions, covering both longitudinal and transverse degrees of freedom. We present here the pseudorapidity multiplicity density per participant pair, and their centrality and energy dependence. Our study reveals a possible violation at $\sqrt{s_{NN}} = 2.76$ TeV of the *limiting fragmentation* observed in multiparticle production of charged particles up to top RHIC energy [39,40]. Predictions for the nuclear modification factors (NMFs) of charged particle (R_{AA}) and of identified particles (R_{AA}^{ID}) are also discussed. We emphasize the role of the SCF effects and gluonic J$\bar{\text{J}}$ loops in understanding the *meson/baryon anomaly* at the LHC energy, which manifests in the (strange) baryon-meson ratios at intermediate and large transverse momenta and in NMFs of identified particles (R_{AA}^{ID}).

II. OUTLINE OF HIJING/B$\bar{\text{B}}$ v2.0 MODEL

A detailed description of the model can be found in Refs. [36–38]. The HIJING model is based on a two-component geometrical model of minijet production and soft interaction and has incorporated nuclear effects such as *shadowing* (nuclear modification of the parton distribution functions) and *jet quenching*, via final state jet medium interaction. In the HIJING/B$\bar{\text{B}}$ v2.0 model [36,37] we introduce new dynamical effects associated with long-range coherent fields (i.e., strong longitudinal color fields, SCFs), including baryon junctions and loops [38,41].

Saturation physics is based on the observation that small-x hadronic and nuclear wave functions, and thus the scattering cross sections as well, are described by the same internal momentum scale known as the *saturation scale* (Q_{sat}) [42]. A recent analysis of pp data up to LHC 7 TeV [43] has shown that, with the k_T factorized gluon fusion approximation the growth of the $dN_{\text{ch}}/d\eta$ can be accounted for if the saturation scale grows with center-of-mass system (c.m.s.) energy as

$$Q_{\text{sat}}^2(s) = Q_0^2(s/s_0)^{\lambda_{\text{CGC}}}, \tag{1}$$

with $\lambda_{\text{CGC}} \approx 0.115$. The saturation scale is also increasing with atomic number as $A^{1/6}$ [44] and it was argued that the effective string tension (κ) of color ropes should scale with Q_{sat}^2 [44,45].

However, in HIJING the string/rope fragmentation is the only soft source of multiparticle production and multiple mini-jets provide a semihard additional source that is computable within collinear factorized standard pQCD with initial and final radiation (DGLAP evolution [46]). In order to achieve a quantitative description, within our HIJING/B$\bar{\text{B}}$ framework we will show that combined effects of hard and soft sources of multiparticle production can reproduce the available data in the range $0.02 < \sqrt{s} < 20$ TeV only with a reduced dependence of the effective string tension on $\sqrt{s}$. We find that the data can be well reproduced taking

$$\kappa(s) = \kappa_0(s/s_0)^{0.06}\text{GeV/fm} \approx Q_{0\kappa}\, Q_{\text{sat}}(s), \tag{2}$$

where $\kappa_0 = 1$ GeV/fm is the vacuum string tension value, $s_0 = 1$ GeV^2 is a scale factor, and $Q_{0\kappa} = \kappa_0/Q_0$ is adjusted to give $\kappa = 1.88$ GeV/fm at the RHIC energy $\sqrt{s} = 0.2$ TeV. Our phenomenological $\kappa(s)$ is compared to $Q_{\text{sat}}^2(s)$ in Fig. 1 from Ref. [36], where $\kappa = 1.40$ GeV/fm at $\sqrt{s} = 0.017$ TeV increases to $\kappa = 3.14$ GeV/fm at $\sqrt{s} = 14$ TeV.

In a strong longitudinal color electric field, the heavier flavor suppression factor $\gamma_{Q\bar{Q}}$ varies with string tension via the well-known Schwinger formula [47],

$$\gamma_{Q\bar{Q}} = \frac{\Gamma_{Q\bar{Q}}}{\Gamma_{q\bar{q}}} = \exp\left(-\frac{\pi\left(M_Q^2 - m_q^2\right)}{\kappa_0}\right) < 1, \tag{3}$$

for $Q = qq$, s, c, or b and $q = u$, d. Therefore, the above formula implies a suppression of heavier quark production according to $u : d : qq : s : c \approx 1 : 1 : 0.02 : 0.3 : 10^{-11}$ for the vacuum string tension $\kappa_0 = 1$ GeV/fm. For a color rope, on the other hand, the *average string tension* value increases due to *in-medium* effect. With these increased string tensions the $Q\bar{Q}$ flavor pair production suppression factors, $\gamma_{Q\bar{Q}}$, approach unity in $A + A$ collisions. In our model this is the main mechanism for strange meson and hyperon enhancement. This increase is quantified in our calculations at RHIC and LHC energies, using a power-law expression,

$$\kappa(s, A)_{\text{RHIC}} = \kappa(s)A^{0.087}, \tag{4}$$

$$\kappa(s, A)_{\text{LHC}} = \kappa(s)A^{0.167}, \tag{5}$$

where the exponent has been fixed to provide a good description of the charged particle densities at mid-pseudorapidity (see below).

Moreover, the measured charged multiplicity grows faster ($\sim \sqrt{s}^{0.3}$) in nucleus-nucleus collisions than it does for protons ($\sim \sqrt{s}^{0.2}$) [48]. The energy dependence of the multiplicity is an experimental probe of possible x dependence of the saturation scale Q_{sat}^2 [49]. Also, the energy density for most central (0%–5%) collisions is larger by about a factor of 3 at LHC than the corresponding one at RHIC [48]. Since the energy densities are computed from the square of the field components [50] they are proportional with $\kappa(s, A)^2$. These experimental facts

indicate that we have to use different exponents at RHIC and at LHC. The problem was also addressed in CGC models, where $Q_{sA}^2 \sim Q_{sp}^2 (A^{1/3})^{1/\gamma_{\rm eff}}$. At smaller x (corresponding to LHC energy) $1/\gamma_{\rm eff}$ is larger, and thus the nuclear enhancement of $Q_{\rm sat}^2$ is expected to be larger than at top RHIC energy [49].

It was shown recently [51] that charged-particle multiplicities measured in central heavy ion collisions at high energies may not directly determine the initial conditions as predicted by CGC models. In its simplest implementation it was generally assumed that there is a direct correspondence between the number of partons in the initial state and the number of particles in the final state [42,43]. However, final-state nonequilibrium production mechanisms generally increase the final multiplicity. In fact, in recent HIJING2.0 (which includes modern structure functions but without SCFs and J$\bar{\rm J}$ loops) the enhancement of the multiplicity due to quenching of final minijets had to be turned off not to overpredict the ALICE $dN_{\rm ch}/dy$ [9]. In HIJING/B$\bar{\rm B}$2.0 used here with supersaturated Duke-Owens parton distribution functions we find a consistent description of both $p+p$ and Pb+Pb multiplicity when taking into account the extra multiplicity generated by minijet quenching.

As mentioned, in HIJING the string/rope fragmentation is the only *soft source* of multiparticle production and multiple minijets provide a semihard additional source that is computable within collinear factorized standard pQCD with initial and final radiation (DGLAP evolution [46]). Within the HIJING model, one assumes that nucleon-nucleon collisions at high energy can be divided into *soft* and *hard* processes with at least one pair of jet production with transverse momentum, $p_T > p_0$. A cutoff (or saturation) scale $p_0(s, A)$ in the final jet production has to be introduced below which the high density of initial interactions leads to a nonperturbative mechanisms which in the HIJING framework is characterized by a finite soft parton cross section $\sigma_{\rm soft}$. The inclusive jet cross section $\sigma_{\rm jet}$ at leading order (LO) [52] is

$$\sigma_{\rm jet} = \int_{p_0^2}^{s/4} dp_T^2 dy_1 dy_2 \frac{1}{2} \frac{d\sigma_{\rm jet}}{dp_T^2 dy_1 dy_2}, \tag{6}$$

where,

$$\frac{d\sigma_{\rm jet}}{dp_T^2 dy_1 dy_2} = K \sum_{a,b} x_1 f_a\left(x_1, p_T^2\right) x_2 f_b\left(x_2, p_T^2\right) \frac{d\sigma^{ab}(\hat{s}, \hat{t}, \hat{u})}{d\hat{t}} \tag{7}$$

depends on the parton-parton cross section σ^{ab} and parton distribution functions (PDFs), $f_a(x, p_T^2)$. The summation runs over all parton species; y_1 and y_2 are the rapidities of the scattered partons; x_1 and x_2 are the light-cone momentum fractions carried by the initial partons. The multiplicative K factor ($K \approx 1.5$–2) accounts for the next-to-leading order (NLO) corrections to the leading order (LO) jet cross section [53,54]. The parton distributions per nucleon in a nucleus (with atomic number A and charge number Z), $f_{a/A}(x, Q^2, r)$, are assumed to be factorizable into parton distributions in a nucleon($f_{N/A}$) and the parton shadowing factor ($S_{a/A}$),

$$f_{a/A}(x, Q^2, r) = S_{a/A}(x, r) f_{N/A}. \tag{8}$$

For the shadowing factor $S_{a/A}$ we take the parametrization used in the regular HIJING model [30,55]. We also take into account the intrinsic transverse momentum and the transverse momentum broadening due to initial multiple scattering.

A saturation in the final state, i.e., of produced gluons, is possible, even without requirement of saturation in the initial state [56]. The largest uncertainty in minijet cross sections is the strong dependence on the minimum transverse momentum scale cutoff, p_0. It was shown that an increased value (with c.m. energy $\sqrt{s}$) is required by the experimental data indicating that the *coherent interaction* becomes important. This might be taken also as an evidence of gluon final state saturation at very small x [9,10]. With the Duke-Owens parametrization [57] of parton distribution functions, an energy-independent cutoff scale $p_0 = 2$ GeV/c and a constant soft parton cross section $\sigma_{\rm soft} = 57$ mb are found to reproduce the experimental data on the hadron central rapidity density in $p + p(\bar{p})$ collisions [36].

However, with a constant momentum cutoff $p_0 = 2$ GeV/c, the total number of minijets per unit transverse area for independent multiple jet production in central nucleus-nucleus collisions could exceed the limit [9,10]

$$\frac{T_{AA}(b)\sigma_{\rm jet}}{\pi R_A^2} \leqslant \frac{p_0^2}{\pi}, \tag{9}$$

where $T_{AA}(b)$ is the overlap function of $A + A$ collisions and π/p_0^2 is the intrinsic transverse size of a minijet with transverse momentum p_0. Therefore, we consider an energy and nuclear size dependent cutoff $p_0(s, A)$, to ensure the applicability of the two-component model in the HIJING model for $A + A$ collisions. The pseudorapidity distribution of charged particles in central nucleus-nucleus collisions at RHIC and LHC energies can well be fitted (see Sec. III A) if we consider a scaling law of the type $C\, A^{\alpha}\, \sqrt{s}^{\beta}$:

$$p_0(s, A) = 0.416\, A^{0.128}\, \sqrt{s}^{\,0.191}\ {\rm GeV}/c. \tag{10}$$

New values for $p_0(s, A)$ increase from $p_0 = 1.5$ GeV/c at the c.m.s. energy $\sqrt{s} = 0.02$ TeV up to $p_0 = 4.2$ GeV/c at $\sqrt{s} = 5.5$ TeV. These values obtained for central $A + A$ collisions are not expected to be valid for peripheral $A + A$ or $p + p$ collisions. These dependencies are similar to those used in pQCD+saturation model from Ref. [58]. The main difference is a factor of two in the constant C, $C_{\rm HIJ} = 0.416$ in comparison with $C_{\rm esk} = 0.208$ from Ref. [58]. Note that $C_{\rm esk} = 0.208$ result in an overestimate of the charged particle density at LHC energies by a factor of approximately two [58].

The above limit for incoherent minijet production should also depend on impact parameter (b) [59]. In the present calculations within our model such dependence is not included. Instead, in the HIJING model an impact-parameter dependence of the gluon shadowing is considered in the parametrization of the parton shadowing factor $S_{a/A}$ [55]. Due to shadowing effects the observed A exponent ($\alpha = 0.128$) is somewhat less than the number expected in the saturated scaling limit [$p_0(s, A) \sim A^{1/6}$] [58].

The ALICE experiment at the LHC published first experimental data on the charged hadron multiplicity density at mid-rapidity in central (0%–5%) Pb+Pb collisions at $\sqrt{s_{NN}} = 2.76$ TeV [17]. In this experiment the collaboration

also confirmed the presence of jet quenching [19] by studying R_{AA}. A measure of the jet quenching at large transverse momentum (p_T) is given by the ratio of particle yield in $A + A$ collisions to that in $p + p$ collisions, defined by

$$R_{AA} = \frac{\left(1/N_{\rm evt}^{AA}\right) d^2 N_{AA}/d^2 p_T dy}{N_{\rm coll}\left(1/N_{\rm evt}^{pp}\right) d^2 N_{pp}/d^2 p_T dy}, \qquad (11)$$

where $N_{\rm evt}$ is the number of events and $N_{\rm coll}$ is the number of binary nucleon-nucleon (NN) collisions. These results provide stringent constraints on the theoretical uncertainties in the bulk hadron production and have important consequences on theoretical predictions for jet quenching in Pb+Pb collisions at LHC energies.

For a parton a, the energy loss per unit distance can be expressed as $dE_a/dx = \epsilon_a/\lambda_a$, where ϵ_a is the radiative energy loss per scattering and λ_a the mean-free path (mfp) of the inelastic scattering. For a *quark jet* at the top RHIC energy $(dE_q/dx)_{\rm RHIC} \approx 1$ GeV/fm and mfp $(\lambda_q)_{\rm RHIC} \approx 2$ fm [37]. The initial parton density is proportional to the final hadron multiplicity density. The charged particle density at mid-pseudorapidity at the LHC is a factor of 2.2 higher than that at the top RHIC energy [17]. Therefore, for a *quark jet* at the LHC the energy loss (mfp) should increase (decrease) by a factor of ≈ 2.0 and become $(dE_q/dx)_{\rm LHC} \approx 2$ GeV/fm and mfp $(\lambda_q)_{\rm LHC} \approx 1$ fm. Throughout this analysis we will consider the results with two sets of parameters for hard interactions:

$(dE/dx)_1$, i.e., $K = 1.5; dE_q/dx = 1\,{\rm GeV/fm}; \lambda_q = 2\,{\rm fm}$ and

$(dE/dx)_2$, i.e., $K = 1.5; dE_q/dx = 2\,{\rm GeV/fm}; \lambda_q = 1\,{\rm fm}$.

Since there is always a coronal region with an average length of λ_q in the system where the produced parton jets will escape without scattering or energy loss, the suppression factor can never be infinitely small. For the same reason, the suppression factor also depends on λ_q. It is difficult to extract information on both dE_q/dx and λ_q simultaneously from the measured spectra in a model-independent way [60]. We show below that a constant radiative energy loss mechanism ($dE/dx = $ const.) as implemented in HIJING/B$\bar{\rm B}$ v2.0 model provides a good description of suppression at intermediate and larger p_T ($4 < p_T < 20\,{\rm GeV}/c$) for charged particle in Pb+Pb collisions at the LHC.

III. RESULTS AND DISCUSSION

A. Multiplicity and centrality dependence

Charged-particle multiplicity density $(2dN_{\rm ch}/d\eta)/N_{\rm part}$ in central (0%–5%) Pb+Pb collisions at $\sqrt{s_{NN}} = 2.76$ TeV reported by the ALICE Collaboration is a factor of 2.2 higher than that observed in central Au+Au collisions at top RHIC energy. This value is larger than most of theoretical predictions, especially those from the CGC models [17]. Such large hadron multiplicity will have important consequences on the estimated *shadowing* and *jet quenching* in Pb+Pb collisions [63]. The value of $(2dN_{\rm ch}/d\eta)/N_{\rm part}$ at mid-pseudorapidity was reproduced by the HIJINGv2.0 model with a new set of PDFs [9] and has helped to constrain the gluon shadowing parameter in the model [10]. However, these calculations

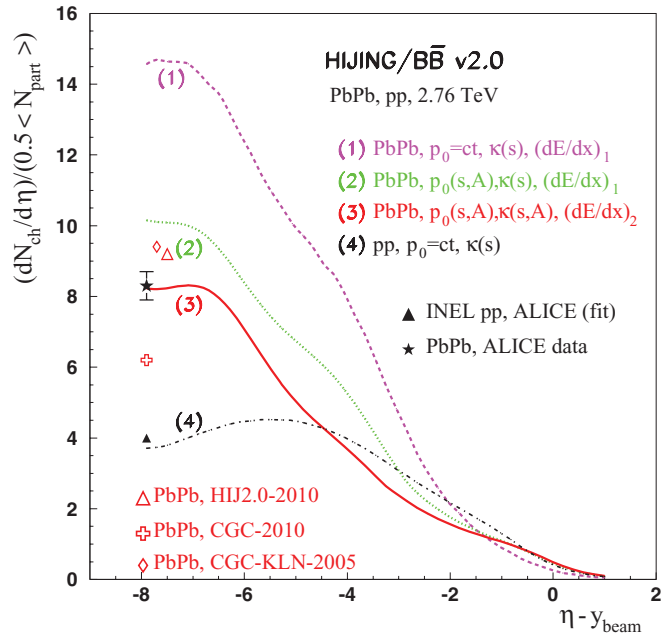

FIG. 1. (Color online) Comparison of HIJING/B$\bar{\rm B}$ v2.0 predictions for $(2dN_{\rm ch}/d\eta)/N_{\rm part}$ in central (0%–5%) Pb+Pb collisions at $\sqrt{s_{NN}} = 2.76$ TeV. The results which give the best fit of the experimental value [17] are plotted as a solid curve. The dotted and dashed curves illustrate the sensitivity to the main model parameters (see Sec. III A for explanation). The dot-dashed curve is obtained for $p + p$ NSD collisions at $\sqrt{s_{NN}} = 2.76$ TeV. The full triangle is the result obtained by interpolating data between 2.36 and 7 TeV in Ref. [18]. Comparisons with other model calculations are also shown: HIJING v2.0 model (open triangle from Ref. [10]), CGC models (open cross from Ref. [6]; open diamond from Ref. [4]).

do not include the effects of *jet quenching*, which has been reported recently by ALICE [19], ATLAS [21], and CMS [22].

In previous studies of heavy-ion collisions at RHIC [36,37], the parameters of the HIJING/B$\bar{\rm B}$ v2.0 model were adjusted in order to reproduce the measured charged particle multiplicity as well as (multi)strange particle production. In the present study of heavy-ion collisions at the LHC we have to modify the values of these parameters in order to fit ALICE data [17]. As shown in Fig. 1 a good description (solid curve) of the measured charged particle multiplicity density at mid-pseudorapidity is obtained if the parameters $p_0(s, A) = 3.7$ GeV/c, $\kappa(s, A) = 6.0$ GeV/fm, and $(dE/dx)_2$ (i.e., $K = 1.5; dE_q/dx = 2$ GeV/fm; $\lambda_q = 1.0$ fm) are used.

The sensitivity of the calculations to the main parameters is illustrated by the dashed, dotted, and solid curves. The dashed curve is obtained with the parameters used at RHIC energies: $p_0 = 2.0\,{\rm GeV}/c, \kappa(s) = 2.6\,{\rm GeV/fm}$, and $(dE/dx)_1$ (i.e., $K = 1.5; dE_q/dx = 1$ GeV/fm; $\lambda_q = 2.0$ fm). The dotted curve is obtained if p_0 is increased to $p_0(s, A) = 3.7\,{\rm GeV}/c$. Changing from set $(dE/dx)_1$ to $(dE/dx)_2$ results in a good description of data (solid curve). The dot-dashed curve is the results for $p + p$ non-single diffractive (NSD) collisions at $\sqrt{s_{NN}} = 2.76$ TeV and are obtained with the same set of parameters as described in Ref. [36].

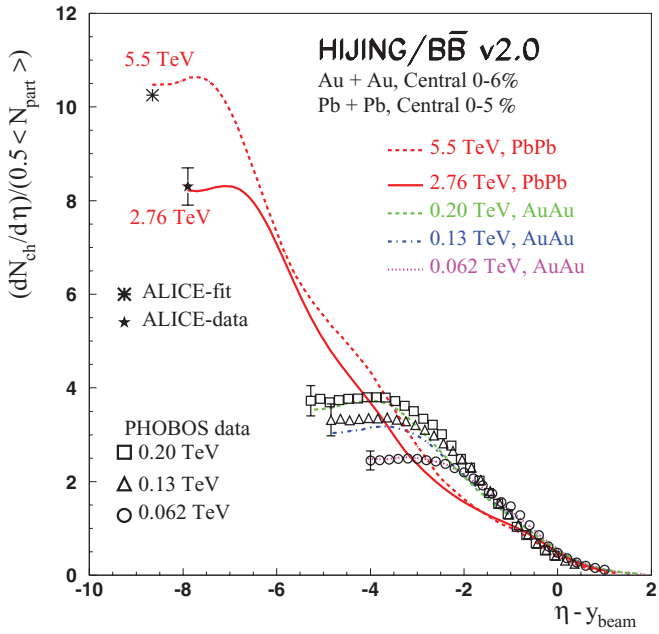

FIG. 2. (Color online) Comparison of HIJING/BB̄ v2.0 predictions for central charged particle density per participant pair produced in $A + A$ collisions at various energies. The data and theoretical results are plotted in the rest frame of one of the nuclei. The Au+Au data are from the PHOBOS Collaboration [39,40]. The statistical error bars are plotted only at mid-pseudorapidity for clarity. The Pb+Pb data at $\sqrt{s_{NN}} = 2.76$ TeV (filled star) are from the ALICE Collaboration [17]. The value at $\sqrt{s_{NN}} = 5.5$ TeV (star) is obtained by a power-law extrapolation from RHIC energies and 2.76 TeV data [17].

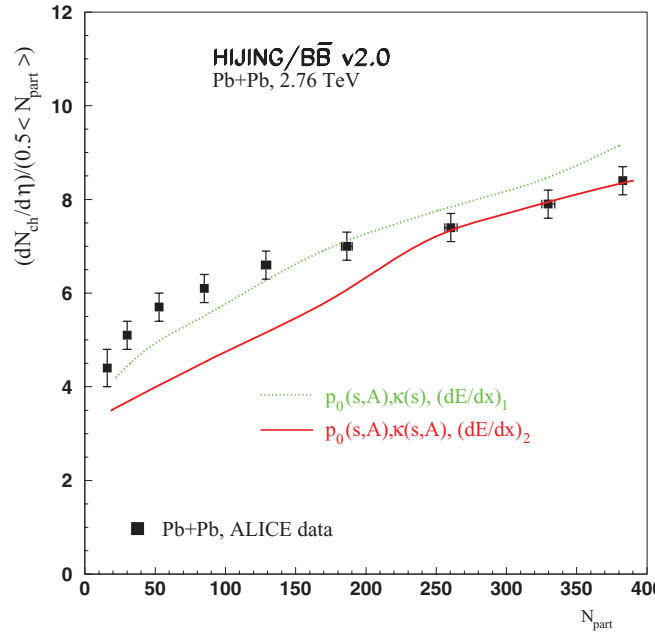

FIG. 3. (Color online) Comparison of HIJING/BB̄ v2.0 model calculations for charged particle multiplicity density at mid-pseudorapidity per participant pair $(2dN_{\rm ch}/d\eta)/N_{\rm part}$ as a function of number of participants in Pb+Pb collisions at $\sqrt{s_{NN}} = 2.76$ TeV. The solid and dotted curves are the results obtained using the same set of parameters as in Fig. 1 (see text for explanations). All calculations include SCF effects and JJ̄ loops. The data are from ALICE Collaboration [18] and the error bars include statistical and systematic uncertainties.

The study of the dependence of observable $(2dN_{\rm ch}/d\eta)/N_{\rm part}$ on the colliding system, center-of-mass energy, and collision geometry is important to understand the relative contributions to particle production of hard scattering and soft processes. Multiparticle production of charged particles at RHIC energies exhibit the phenomenon of *limiting fragmentation* [39,40]. This phenomenon is a consequence of Feynman scaling (if one views the collision in the rest frame of one of the incident particles, the production process of the soft particles is independent of the energy or rapidity of the other particle.). The region in rapidity over which the particles appears to be independent of energy increases with energy. It was argued that this phenomenon (called *extended longitudinal scaling*) is a direct manifestation of initial saturation which is assumed in CGC models [40].

Figure 2 displays the results for central (0%–6%) Au+Au collisions at RHIC energies (0.062 TeV $< \sqrt{s_{NN}} <$ 0.20 TeV) and in central (0%–5%) Pb+Pb collisions at LHC energies ($\sqrt{s_{NN}} = 2.76$ TeV and $\sqrt{s_{NN}} = 5.5$ TeV). Our calculations show that at RHIC energies the model predicts approximately a scaling seen also in data. However, some degree of violation of the phenomenon of *limiting fragmentation* and of the *extended longitudinal scaling* is predicted at both LHC energies. This violation is due to the parton hard scattering included in our model and missing in CGC models [3,4,6,43].

Figure 3 shows the dependence of the pseudorapidity densities $(2dN_{\rm ch}/d\eta)/N_{\rm part}$ at mid-pseudorapidity on the number of participants as measured by the ALICE Collaboration. The charged-particle density normalized per participant pair increases by a factor of roughly two from peripheral (70%–80%) to central (0%–5%) Pb+Pb collisions. The model calculations which have been tuned to high-energy $p + p$ [36] and central (0%–5%) Pb+Pb collision data reasonably describe the central Pb+Pb data for $N_{\rm part} > 250$. However, with the same set of parameters the model predicts a stronger rise with centrality than observed.

For peripheral collisions a better description is obtained if one use as parameters for the soft part $\kappa(s)$ [instead of $\kappa(s, A)$], successful in describing $p + p$ collisions, and for hard scattering $p_0(s, A)$, $(dE/dx)_1$, as deduced from RHIC data. However, in this scenario the model overpredicts the absolute magnitude for central collisions ($N_{\rm part} > 250$). These results indicate that the average energy loss per unit distance and the effective string tension values should have an impact parameter (b) and a parton density dependence, and a fine-tuning is required to describe better these data. We leave this study to a future analysis.

B. Nuclear modification factor for charged particle

In this paper, we make a simultaneous analysis of the high and low p_T part of charged-hadron p_T spectrum. Experiments

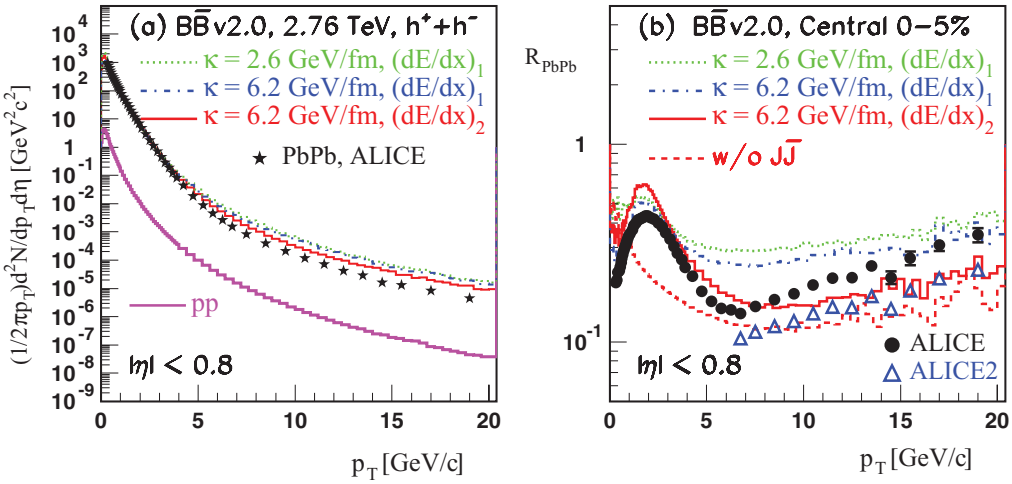

FIG. 4. (Color online) (a) Comparison of HIJING/B$\bar{\text{B}}$ v2.0 predictions for the p_T distributions of primary charged particles at mid-pseudorapidity ($-0.8 < \eta < 0.8$) in central (0%–5%) Pb+Pb collisions at $\sqrt{s_{NN}} = 2.76$ TeV. Theoretical calculations are for different values of parameters (see text for explanations). The $p + p$ references values are shown as the lower solid histogram. (b) Theoretical calculations for nuclear modification factors R_{AA} are compared to data. The data (left and right panels) are from the ALICE Collaboration [19]. Error bars are statistical only. In part (b) the open triangles are the results for R_{AA} at $p_T > 6.5$ GeV/c using alternative $p + p$ reference spectrum [19].

at RHIC energies reported a suppression by a factor ≈5 compared with expectations from an independent superposition of nucleon-nucleon (*NN*) collisions [61,62], interpreted as strong evidence of formation of a strong-coupling QGP (sQGP) in $A + A$ collisions. The jet quenching has also been confirmed in central (0%–5%) Pb+Pb collisions at the LHC [19,21,22].

Having a good description for charged particle multiplicity at mid-pseudorapidity, we analyze the model predictions on suppression of single hadron spectra in central (0%–5%) Pb+Pb collisions at the LHC. For other recent works discussing NMFs of charged particles (R_{AA}) at the LHC, see recent references [63–69]. At the higher LHC energies a larger density of the medium is expected. This should lead to a larger suppression compared with that seen at RHIC energies. The observed nuclear modification factor R_{AA} [19] is characterized by the following behavior: a maximum at approximately $p_T = 2$ GeV/c and a decrease with increasing p_T in the range 2–6 GeV/c. For p_T greater that 6 GeV/c, R_{AA} rises to reach a value of ≈ 0.4 at $p_T \approx 20$ GeV/c.

The measured and predicted transverse momentum spectra at mid-pseudorapidity of primary charged particles in central (0%–5%) Pb+Pb collisions (upper solid histogram) and in $p + p$ collisions (lower solid histogram) at $\sqrt{s_{NN}} = 2.76$ TeV are compared in Fig. 4(a). The HIJING/B$\bar{\text{B}}$ v2.0 model describes fairly well the experimental p_T spectrum reported in Ref. [19]. The sensitivity of the calculations to the effective value of the string tension (κ) is shown by comparing the dotted [$\kappa(s) = 2.6$ GeV/fm] and the dashed [$\kappa(s, A) = 6.2$ GeV/fm] histograms. The sensitivity to the main hard scattering parameters is seen by comparing the results obtained with the two sets $(dE/dx)_2$ (solid histograms) and $(dE/dx)_1$(dash-dotted histograms). However, with the best set of parameters (solid histograms) the model still overestimates the high p_T tail of the p_T spectra. There are no experimental data on charged hadron spectra in $p + p$ collisions at $\sqrt{s_{NN}} = 2.76$ TeV. ALICE data on the suppression factor (R_{AA}) were obtained using a $p + p$ spectrum interpolated from their data at 0.9 TeV and 7 TeV. The open triangles in Fig. 4(b) represent the uncertainty in the interpolation method (see Ref. [19] for more details).

In medium modification of NMFs R_{AA} is mainly caused by the energy loss suffered by partons while transversing the plasma due to collisions and radiation of gluons before they fragment and by the nuclear shadowing. To describe the nuclear shadowing we use in Eq. (8) the same functions as those used in the regular HIJING model [30]. This has been shown to be successful in explaining the results for R_{AA} at RHIC energies [37,38]. The benchmark of any theoretical calculation is to describe the shape seen at low $p_T < 6$ GeV/c in R_{AA}. We can explain the shape and the presence of a maximum at approximately $p_T = 2$ GeV/c as a specific interplay between nonperturbative (SCF effects) and perturbative (gluonic J$\bar{\text{J}}$ dynamical loops) mechanism contributions. The results without J$\bar{\text{J}}$ loops (dashed histogram) shown in Fig. 4(b) strongly underestimate the experimental values of R_{AA} in this p_T range.

Since we are mostly interested in the overall effects, we concentrate also on the modification of high p_T hadron spectra due to an assumed total energy loss related to the averaged energy loss per unit distance. The mechanism which gives a constant energy loss per collisions is seen to describe quite well the data (within the systematics uncertainties) over the largest p_T window of 6–20 GeV/c. R_{AA} increases with p_T because of the constant energy loss assumed here. For a constant energy loss per collisions (ΔE_T) the ratio $\Delta E_T/E_T$ becomes smaller for larger E_T, and thus the suppression is expected to decrease with increasing p_T. Here, the energy loss per collisions is about twice as large and the mean-free path of parton-parton interactions is smaller by a factor of roughly two as compared with that used at the top RHIC energy. These analyses can provide information about the average total energy loss the parton suffers during its interaction with the medium. However, a more quantitative analysis should be

performed with the knowledge of the dynamical evolution of the system which is beyond the scope of this paper.

C. Baryon/meson anomaly at the LHC

Identified particles at high p_T provide direct sensitivity to differences between quark and gluon fragmentation [70]. Proton and pion production at high p_T is expected to have significant contributions from quark fragmentation while antiprotons result mainly from gluon fragmentation [60]. Therefore, the ratios $\bar{p}/\pi^-$, p/π^+ are sensitive to the possible color charge dependence of energy loss. Systematic measurements of identified particle spectra in $p+p$ and Au+Au collisions at RHIC energies [70–74] in the p_T region 2–12 GeV/c show a significant suppression with respect to binary scaling. However, protons and antiprotons are less suppressed than pions at intermediate p_T (2–9 GeV/c). For $p_T > 2$ GeV/c, the ratios $\bar{p}/\pi^-$ and p/π^+ do not depend strongly on energy and they are higher in central than in peripheral collisions. In addition to being sensitive to quark and gluon jet production these are also sensitive to baryon transport properties and the energy density.

Moreover, the meson/baryon ratio suggest that baryon and antibaryon production may dominate the moderate high p_T flavor yields. These findings challenge various models incorporating jet quenching [60,75], and/or constituent quark coalescence [76,77]. The fact that in the intermediate p_T region the p/π^+ and $\bar{p}/\pi^-$ ratios are close to unity (baryon/meson anomaly) has been attributed to either quark coalescence or to novel baryon transport dynamics [75], based on topological gluon field configurations [78–81]. However, the baryon junction model predictions from Ref. [75] are not in agreement with data [72].

Figure 5 displays the mid-rapidity ratios for central (0%–12%) Au+Au collisions [72] at $\sqrt{s_{NN}} = 0.2$ TeV in comparison with model predictions. The observed ratios peak at $p_T \approx 2$–3 GeV/c with value close to unity and then decrease with increasing p_T and approach the ratios observed in $p+p$ collisions at $p_T > 6$ GeV/c. The results presented (solid histograms) include SCF and $J\bar{J}$ loops contributions. The calculations based on quark coalescence (dot-dashed curves) and thermal models (dotted curves) from Ref. [76] are also plotted. The grouping of particle production according to the number of constituent quarks has been attributed to quark coalescence from a collective partonic medium [77]. The coalescence models [76,77] can qualitatively describe these data at intermediate $p_T < 5$ GeV/c, but strongly underpredict the results at high p_T, due to fragmentation functions used within the model. To the contrary, the thermal model calculations [76] strongly overestimate the data at high p_T. Our model provides an alternative explanation to the baryon/meson anomaly. The reason is a specific interplay of contributions from SCF effects and dynamical $J\bar{J}$ loops. The predictions of our model are in good agreement with data up to the highest p_T, in the limit of systematics uncertainties. However, the model overestimates the p/π^+ ratio for $3 < p_T < 6$ GeV/c; while it provides a good description for protons (p), it underpredicts the pion (π^+) spectrum in this region. Since the ratio $\bar{p}/\pi^-$ is well described by the model, these calculations could indicate that the fragmentation functions for π^+ production are not well estimated.

With the best set of parameters used to describe charged particle production in central (0%–5%) and peripheral (70%–80%) Pb+Pb collisions at $\sqrt{s_{NN}} = 2.76$ TeV (see Sec. III A), we present in Fig. 6 the model predictions for centrality dependence of the nonstrange baryon/meson ratio (left panel) and of the strange baryon/meson ratio (right panel). Our model predicts that these ratios do not depend strongly on energy and centrality. The model also predicts that the baryon/meson anomaly will persist up to high p_T. For central (0%–5%) Pb+Pb collisions at $\sqrt{s_{NN}} = 2.76$ TeV, in a scenario with jet quenching and shadowing as explained in Sec. II, but without $J\bar{J}$ loops and SCF effects, the $\bar{p}/\pi^-$ ratio in the region of the maximum ($2 < p_T < 3$ GeV/c) is 0.07. We have studied the sensitivity of the results to the $J\bar{J}$ loops and SCF effects. Considering only $J\bar{J}$ loops leads to an increase by a factor of two, and taking into consideration only SCF effects leads to an increase of up to a factor of ≈14 for the $\bar{p}/\pi^-$ ratio.

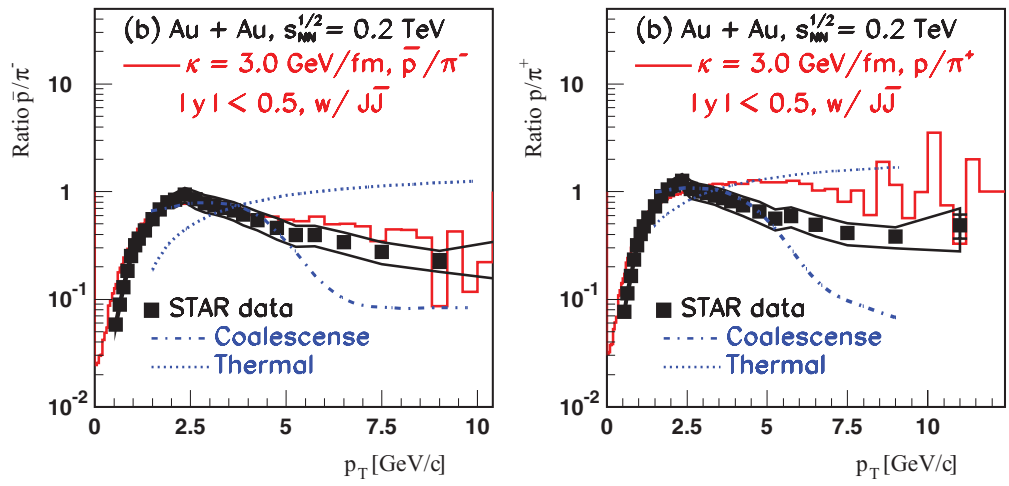

FIG. 5. (Color online) Comparison of HIJING/B$\bar{B}$ v2.0 predictions (solid histogram) for ratios $\bar{p}/\pi^-$ (left panel) and p/π^+ (right panel) to STAR data [72] and to coalescence (dot-dashed curves) and thermal (dotted curves) model calculations from Ref. [76]. The error bars include only statistical uncertainties and systematics are introduced by thin continuous curves.

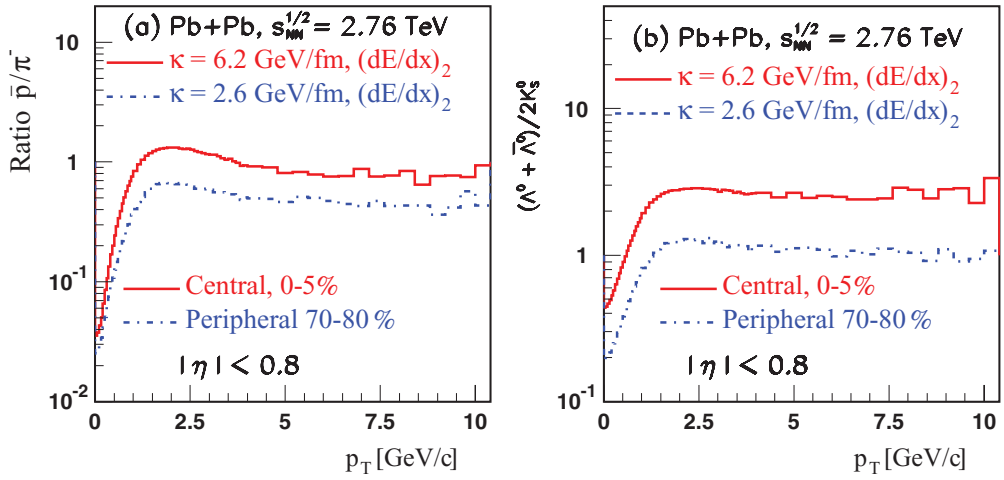

FIG. 6. (Color online) Predictions for centrality dependence of (non)strange baryon/meson ratios from HIJING/B$\bar{\text{B}}$ v2.0. The results include SCF effects and J$\bar{\text{J}}$ loops. In each figure the histograms correspond to two value of centrality and the associated string tension.

Note that an important fraction of this increase is also due to much stronger quench of pions in comparison with that of antiprotons, as we will show below (see Fig. 8).

The ALICE and CMS detectors are designed to perform measurements in the high-multiplicity environment of central Pb+Pb collisions at the LHC [34,35]. To isolate QGP signatures in heavy-ion collisions, understanding the particle production properties from NN interactions is necessary. In addition, the transverse momentum spectrum in $p + p$ collisions serves as a baseline to study possible suppression [i.e., nuclear modification factor $R_{AA}^{\text{ID}}(p_T)$] in heavy-ion collisions. This stresses the need for reference $p + p$ measurements at LHC energies of identified particles. In a previous paper [36] we show that the large (strange) baryon-to-meson ratios measured at Tevatron (1.8 and 1.96 TeV) and LHC energies (0.9 and 7 TeV) are well described in the framework of the HIJING/B$\bar{\text{B}}$ v2.0 model. Recently, the CDF reported a set of measurements of inclusive invariant p_T differential cross sections of hyperons with different strangeness, Λ^0 [quark content (uds)], Ξ^- (dss), and Ω (sss). These data are obtained for the central region with pseudorapidity range $-1 < \eta < 1$ and p_T up to 10 GeV/c, and are used to test our model calculations which include SCF effects and J$\bar{\text{J}}$ loops.

In a scenario with SCF effects (i.e., considering $\kappa = \kappa(s)$ [36]) the increase of the yield is higher for multistrange hyperons (Ξ^-,Ω^-) than for the strange hyperon (Λ^0), in comparison with the results obtained without SCF effects (i.e., taking vacuum string tension value $\kappa_0 = 1$ GeV/fm). The increase of the yield with strangeness content is due to an increase of strange quark suppression (γ_s), obtained from a power-law dependence of effective string tension values, $\kappa(s) = \kappa_0\ (s/s_0)^{0.06}$ GeV/fm (see Fig. 2 from Ref. [36]).

Figure 7 shows the predicted p_T differential cross sections (left panel) for the three hyperon resonances in comparison with data. The plots on the right side of Fig. 7 show the ratio of the p_T differential cross sections for Ξ^-/Λ^0 and Ω^-/Λ^0.

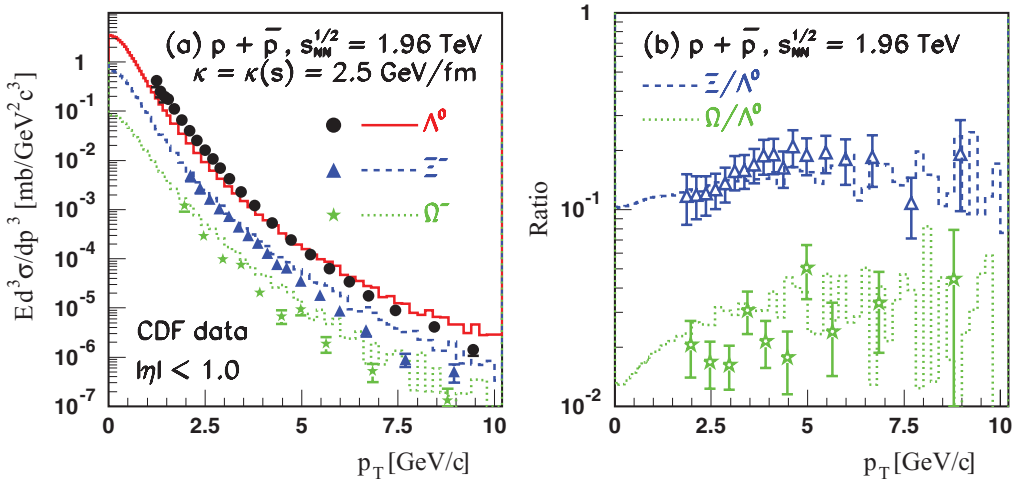

FIG. 7. (Color online) (a) Comparison of HIJING/B$\bar{\text{B}}$ v2.0 predictions for the P_T differential cross sections of Λ^0 (solid), Ξ (dashed), and Ω (dotted histograms). The calculations are for $p + \bar{p}$ collisions at 1.96 TeV and include SCF effects and J$\bar{\text{J}}$ loops as in Ref. [36]. (b) The ratios Ξ/Λ^0 (dashed histogram) and Ω/Λ^0 (dotted histogram). The data are from the CDF Collaboration [33]. Only statistical uncertainties are shown.

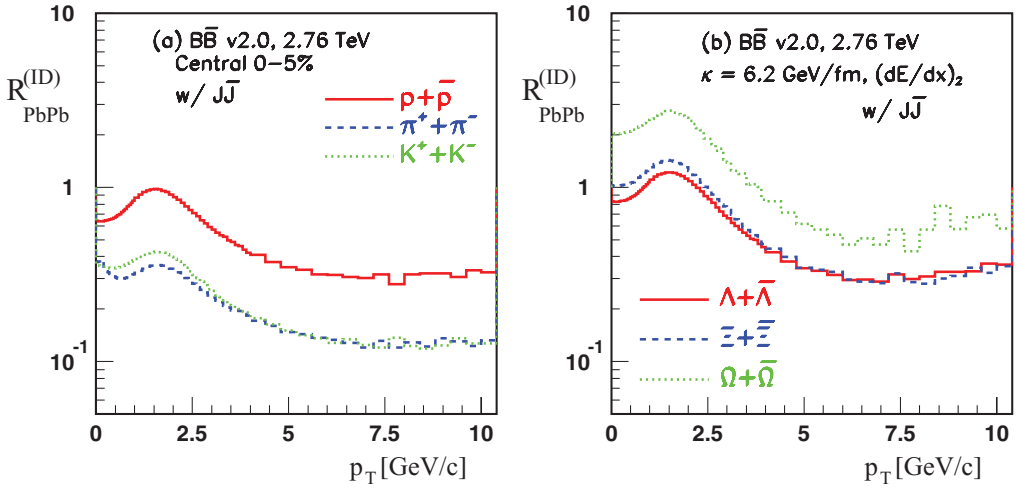

FIG. 8. (Color online) Predictions from HIJING/BB̄ v2.0 model for nuclear modification factors $R_{AA}^{\rm ID}$ of identified particles at mid-pseudorapidity ($-0.8 < \eta < 0.8$) in central (0%–5%) Pb+Pb collisions at $\sqrt{s_{NN}} = 2.76$ TeV. The results include SCF effects and JJ̄ loops. Left: pions, kaons, and protons. Right: hyperons Λ, Ξ, Ω.

In the limit of the experimental error (systematics+statistical) our model describes well these data.

Strangeness enhancement, strong baryon transport, and increase of intrinsic transverse momentum are all expected consequences of longitudinal SCF effects. These are modeled in our microscopic models as an increase of the effective string tension that controls quark-antiquark ($q\bar{q}$) and diquark-antidiquark ($qq\overline{qq}$) pair creation rates and the strangeness suppression factors (γ_s). The predictions in central Pb+Pb collisions for initial energy density and temperature are $\epsilon_{\rm LHC} \approx 200$ GeV/fm^3 and $T_{\rm LHC} \approx 500$ MeV, respectively [82]. Both values would lead in the framework of our model to an estimated increase of the average value of string tension to $\kappa_{\rm LHC} \approx 5$–$6$ GeV/fm [2], consistent with our parametrization from Eq. (5).

The predictions for NMFs of identified particles [$R_{AA}^{\rm ID}(p_T)$] are presented in Fig. 8 for nonstrange particles (left panel) and (multi)strange particles (right panel). From the results of our model we conclude that the baryon/meson anomaly, i.e., different meson and baryon suppression, will persist in central Pb+Pb collisions at the LHC energy $\sqrt{s_{NN}} = 2.76$ TeV up to a higher value of transverse momentum. The $R_{AA}^{\rm ID}(p_T)$ also exhibit an ordering with strangeness content at low and intermediate p_T, the increase of the yield being higher for multistrange hyperons than that for (non)strange baryons [i.e., $R_{\rm PbPb}(\Omega) > R_{\rm PbPb}(\Xi) > R_{\rm PbPb}(\Lambda) > R_{\rm PbPb}(p)$]. This prediction could be verified by the future planned experiments at the LHC.

IV. SUMMARY AND CONCLUSIONS

We have studied the influence of strong longitudinal color fields and of possible multigluon JJ̄ loops dynamics in particle production in Pb+Pb collisions at 2.76 TeV. We have investigated a set of observables sensitive to the dynamics of the collisions, covering both longitudinal and transverse degree of freedom. A detailed comparison with available experimental data from the LHC has been performed.

We find that the inclusion of the multiple minijet source limits the growth of the string tension $\kappa(s)$ to be approximately linear as a function of saturation scale $Q_{\rm sat}$, in contrast to recent approaches [43] where $\kappa(s)$ scales as $Q_{\rm sat}^2$. The reason is that in the CGC model the collinear factorized minijet mechanism is suppressed by geometric scaling to much higher p_T. Moreover, an increase with A due to an increase in initial energy density is necessary in order to better describe new ALICE data.

We have shown that strong color field (SCF) could play an important role in particle production at mid-rapidity in heavy-ion collisions. The mechanisms of hadron production are very sensitive to the early phase of the collisions, when fluctuations of the color field strength are highest. Strong color field effects are modeled by varying the effective string tension that controls the quark-antiquark ($q\bar{q}$) and diquark-antidiquark ($qq\overline{qq}$) pair creation rates and strangeness suppression factors (γ_s). SCF also modify the fragmentation processes resulting in an increase of (strange) baryons.

We show that the baryon/meson anomaly manifests in an increase of baryon-to-meson ratios as well as in different suppression of mesons and baryons and persists up to high p_T ($p_T < 10$ GeV/c). We show also that the $R_{AA}^{\rm ID}(p_T)$ exhibit an ordering with strangeness content at low and intermediate p_T, the increase of the yield being higher for multistrange hyperons than that for (non)strange baryons.

ACKNOWLEDGMENTS

We thank S. Das Gupta, S. Jeon, and P. Levai for fruitful discussions and support. V.T.P. acknowledges the use of computer facilities at Columbia University, New York, where part of these calculations were performed. This work was supported by the Natural Sciences and Engineering Research Council of Canada. This work was also supported by the Division of Nuclear Science, of the U.S. Department of Energy, under Contract No. DE-AC03-76SF00098 and DE-FG02-93ER-40764.

[1] N. Armesto *et al*., J. Phys. G **35**, 054001 (2008).
[2] N. Armesto *et al*., J. Phys. G **35**, 054001 (2008); V. Topor Pop, J. Barrette, C. Gale, S. Jeon, and M. Gyulassy, *ibid*. **35**, 15 (2008); **35**, 57 (2008).
[3] J. L. Albacete, J. Phys. Conf. Ser. **270**, 012052 (2011).
[4] D. Kharzeev, E. Levin, and M. Nardi, Nucl. Phys. A **747**, 609 (2005).
[5] N. Armesto, C. A. Salgado, and U. A. Wiedemann, Phys. Rev. Lett. **94**, 022002 (2005).
[6] E. Levin and A. H. Rezaeian, Phys. Rev. D **82**, 054003 (2010).
[7] E. Levin and A. H. Rezaeian, Phys. Rev. D **82**, 014022 (2010).
[8] E. Levin and A. H. Rezaeian, Phys. Rev. D **83**, 114001 (2011).
[9] W.-T. Deng, X.-N. Wang, and R. Xu, Phys. Rev. C **83**, 014915 (2011).
[10] W.-T. Deng, X.-N. Wang, and R. Xu, Phys. Lett. B **701**, 133 (2011).
[11] P. Bozek, M. Chojnacki, W. Florkowski, and B. Tomasik, Phys. Lett. B **694**, 238 (2010).
[12] E. K. G. Sarkisyan and A. S. Sakharov, Eur. Phys. J. C **70**, 533 (2010).
[13] T. J. Humanic, arXiv:1011.0378.
[14] J. Xu and C. M. Ko, Phys. Rev. C **83**, 034904 (2011).
[15] M. Mitrovski, T. Schuster, G. Graf, H. Petersen, and M. Bleicher, Phys. Rev. C **79**, 044901 (2009).
[16] F. W. Bopp, R. Engel, J. Ranft, and S. Roesler, arXiv:0706.3875.
[17] K. Aamodt *et al*. (ALICE Collaboration), Phys. Rev. Lett. **105**, 252301 (2010).
[18] K. Aamodt *et al*. (ALICE Collaboration), Phys. Rev. Lett. **106**, 032301 (2011).
[19] K. Aamodt *et al*. (ALICE Collaboration), Phys. Lett. B **696**, 30 (2011).
[20] K. Aamodt *et al*. (ALICE Collaboration), Phys. Rev. Lett. **105**, 252302 (2010).
[21] G. Aad *et al*. (ATLAS Collaboration), Phys. Rev. Lett. **105**, 252303 (2010).
[22] S. Khachatryan *et al*. (CMS Collaboration), arXiv:1102.1957.
[23] J. Casalderrey-Solana, J. G. Milhano, and U. A. Wiedemann, J. Phys. G **38**, 035006 (2011).
[24] M. H. Seymour, to be published in the Proceedings of Physics at LHC 2010 (PHLC2010), 7–12 June 2010, Hamburg, Germany, arXiv:1008.2927.
[25] R. Sassot, P. Zurita, and M. Stratmann, Phys. Rev. D **82**, 074011 (2010).
[26] K. Werner, I. Karpenko, and T. Pierog, Phys. Rev. Lett. **106**, 122004 (2011).
[27] B. Andersson, G. Gustafson, and B. Nilsson-Almqvist, Nucl. Phys. B **281**, 289 (1987); B. Nilsson-Almqvist and E. Stenlund, Comput. Phys. Commun. **43**, 387 (1987).
[28] A. Capella, U. Sukhatme, and J. Tran Thanh Van, Z. Phys. C **3**, 329 (1979); J. Ranft, Phys. Rev. D **37**, 1842 (1988).
[29] H.-U. Bengtsson and T. Sjostrand, Comput. Phys. Commun. **46**, 43 (1987).
[30] X.-N. Wang and M. Gyulassy, Comput. Phys. **83**, 307 (1994); X.-N. Wang, Phys. Rep. **280**, 287 (1997).
[31] P. Koch, B. Muller, and J. Rafelski, Phys. Rep. **142**, 321 (1986).
[32] A. Andrighetto *et al*. (WA85 and WA94 Collaborations), J. Phys. G **25**, 209 (1999).
[33] T. Aaltonen *et al*. (CDF Collaboration), arXiv:1101.2996.
[34] K. Aamodt *et al*. (ALICE Collaboration), Eur. Phys. J. C **71**, 1655 (2011).
[35] V. Khachatryan *et al*. (CMS Collaboration), J. High Energy Phys. 1105 (2011) 064.
[36] V. Topor Pop, M. Gyulassy, J. Barrette, C. Gale, and A. Warburton, Phys. Rev. C **83**, 024902 (2011).
[37] V. Topor Pop, M. Gyulassy, J. Barrette, C. Gale, S. Jeon, and R. Bellwied, Phys. Rev. C **75**, 014904 (2007), and references therein.
[38] V. Topor Pop, M. Gyulassy, J. Barrette, and C. Gale, Phys. Rev. C **72**, 054901 (2005).
[39] W. Busza *et al*. (PHOBOS Collaboration), Nucl. Phys. A **830**, 35c (2009).
[40] W. Busza, Nucl. Phys. A **854**, 57 (2011).
[41] G. Ripka, editor, *Dual Superconductor Models of Color Confinement*, Lecture Notes in Physics 639 (Springer, Berlin, 2004).
[42] F. Gelis, T. Lappi, and L. McLerran, Nucl. Phys. A **828**, 149 (2009); T. Lappi and L. McLerran, *ibid*. **772**, 200 (2006).
[43] Larry McLerran and Michal Praszalowicz, Acta Phys. Pol. B **41**, 1917 (2010).
[44] D. Kharzeev, E. Levin, and K. Tuchin, Phys. Rev. C **75**, 044903 (2007).
[45] N. Tanji, Ann. Phys. (NY) **324**, 1691 (2009).
[46] G. Altarelli and G. Parisi, Nucl. Phys. B **126**, 298 (1977).
[47] J. S. Schwinger, Phys. Rev. **82**, 664 (1951).
[48] A. Troia *et al*. (ALICE Collaboration), arXiv:1107.1973.
[49] T. Lappi, Eur. Phys. J. C **71**, 1699 (2011).
[50] N. Cardoso, M. Cardoso, and P. Bicudo, arXiv:1108.1542.
[51] R. Baier, A. H. Mueller, D. Schiff, and D. T. Son, arXiv:1103.1259.
[52] E. Eichten, I. Hinchliffe, K. D. Lane, and C. Quigg, Rev. Mod. Phys. **56**, 579 (1984); **58**, 1065 (1986).
[53] K. J. Eskola and X.-N. Wang, Int. J. Mod. Phys. A **10**, 3071 (1995).
[54] J. M. Campbell, J. W. Huston, and W. J. Stirling, Rep. Prog. Phys. **70**, 89 (2007).
[55] X.-N. Wang and M. Gyulassy, Phys. Rev. Lett. **68**, 1480 (1992).
[56] K. J. Eskola, Nucl. Phys. A **698**, 78c (2002).
[57] D. W. Duke and J. F. Owens, Phys. Rev. D **30**, 49 (1984).
[58] K. J. Eskola, K. Kajantie, P. V. Ruuskanen, and K. Tuominen, Nucl. Phys. B **570**, 379 (2000).
[59] K. J. Eskola, K. Kajantie, and K. Tuominen, Phys. Lett. B **497**, 39 (2001).
[60] X.-N. Wang, Phys. Rev. C **58**, 2321 (1998).
[61] J. Adams *et al*. (STAR Collaboration), Nucl. Phys. A **757**, 102 (2005).
[62] K. Adcox *et al*. (PHENIX Collaboration), Nucl. Phys. A **757**, 184 (2005).
[63] X.-F. Che, T. Hirano, E. Wang, X.-N. Wang, and H. Zhang, arXiv:1102.5614.
[64] A. Majumder and C. Shen, arXiv:1103.0809.
[65] T. Renk, H. Holopainen, R. Paatelainen, and K. J. Eskola, Phys. Rev. C **84**, 014906 (2011).
[66] A. Kormilitzin, E. Levin, and A. H. Rezaeian, Nucl. Phys. A **860**, 84 (2011).
[67] D. K. Srivastava, J. Phys. G **38**, 055003 (2011).
[68] W. A. Horowitz and M. Gyulassy, arXiv:1104.4958.
[69] P. Levai, Nucl. Phys. A **862–863**, 146 (2011).
[70] B. I. Abelev *et al*. (STAR Collaboration), Phys. Rev. Lett. **97**, 152301 (2006).
[71] B. I. Abelev *et al*. (STAR Collaboration), Phys. Rev. C **79**, 034909 (2009).

[72] B. I. Abelev *et al*. (STAR Collaboration), Phys. Lett. B **655**, 104 (2007).
[73] S. S. Adler *et al*. (PHENIX Collaboration), Phys. Rev. Lett. **91**, 172301 (2003).
[74] J. Adams *et al*. (STAR Collaboration), Phys. Rev. Lett. **92**, 052302 (2004).
[75] I. Vitev and M. Gyulassy, Phys. Rev. C **65**, 041902 (2002).
[76] R. J. Fries, B. Muller, C. Nonaka, and S. A. Bass, Phys. Rev. C **68**, 044902 (2003).
[77] R. J. Fries, V. Greco, and P. Sorensen, Annu. Rev. Nucl. Part. Sci. **58**, 177 (2008), and references therein.
[78] G. C. Rossi and G. Veneziano, Nucl. Phys. B **123**, 507 (1977).
[79] L. Montanet, G. C. Rossi, and G. Veneziano, Phys. Rept. **63**, 149 (1980).
[80] D. Kharzeev, Phys. Lett. B **378**, 238 (1996).
[81] S. E. Vance and M. Gyulassy, Phys. Rev. Lett. **83**, 1735 (1999).
[82] B. Muller, Nucl. Phys. A **783**, 403 (2007).